Proc. Camb. Phil. Soc. (1970), **68**, 547
PCPS 68–59
With 18 *text-figures*
Printed in Great Britain

The Rikitake two-disc dynamo system

By A. E. COOK† and P. H. ROBERTS‡

(*Received* 6 *August* 1969)

Abstract. It is shown that the solution of the Rikitake two-disc dynamo system may be described by an orbiting point which, for sufficiently large time, lies arbitrarily close to a limit surface of bounded area. Reversal of the field currents of the dynamo coils are shown to occur in the juxtaposed regions of the two sheets of the limit surface. The two singular points of the system are shown, by Liapounov's direct method, to be unstable foci. An asymptotic theory is developed for the case of small difference in dynamo velocities; the theory is applied to cases of small dissipation in which orbits tend to become nearly periodic with a single oscillation between reversals.

1. *Introduction.* The palaeomagnetic record contains evidence that the Earth's dipole has reversed its polarity many times in an irregular manner, and the archeomagnetic results indicate that, even while of one sign, its magnitude fluctuates. Data obtained from ocean cores covering the past ten million years were presented and thoroughly discussed by Cox(1), who proposed a statistical model of the polarity intervals. He divided the reversals into 'polarity epochs', when the interval between successive reversals is of the order of a million years, and 'polarity events', for intervals of 10^4 to 10^5 years. Over the past four million years there have been at least sixteen such intervals, of which seven are polarity events and nine polarity epochs. The statistics of reversals do not appear to have changed appreciably over the last ten million years. Over a wider time interval, however, some variability is evident: for example, there have been no reversals recorded for the seventy million years of the Permian (see Irving(2)).

It is now generally believed that the irregularity of the reversals must be an inherent feature of the Earth's magnetohydrodynamic dynamo rather than the result of vagaries in the dynamical forces acting on the core. Because of the complexity of this non-linear mechanism, homopolar disc dynamos have been proposed as possible analogies. Bullard(3) introduced and studied a single self-excited disc dynamo system, but found that reversals were not possible for such a system. Rikitake(4) discussed the case of two identical coupled disc dynamos in which the current from each disc energizes the coil of the other. He found, by numerical integration, that it was possible for the currents to reverse sign. More recently, Allan(5) confirmed by numerical integration the reversal property of the Rikitake two-disc dynamo system. Although

† Teeside Polytechnic, Middlesbrough.
‡ Newcastle University School of Mathematics, Newcastle-upon-Tyne.

https://doi.org/10.1017/S0305004100046338 Published online by Cambridge University Press

his integrations were much more extensive in time than those of Rikitake, he was only able to give the broad features of the actual reversal process. Somerville(6), in a summary of Allan's paper and his own extensions of it, stated:

'... it is clear that even the simplest coupled dynamo systems are presently very imperfectly understood.'

Results given in the present paper are based on extensive integrations in time using numerical and analogue methods. The topology of the set of trajectories of the solutions in phase space is determined for a range of the fundamental parameter μ, representing ohmic dissipation. It is shown that the topological presentation considerably clarifies the nature of the reversal process. The stability of the trajectories near the stationary points is examined using Liapounov's second method. It is found that for all physically realistic μ and K the trajectories are unstable. A relation between the period of oscillation and maximum current excursion is developed for the case of small difference in angular velocity, A. For very small dissipation, the trajectories are almost periodic, having a single oscillation between reversals.

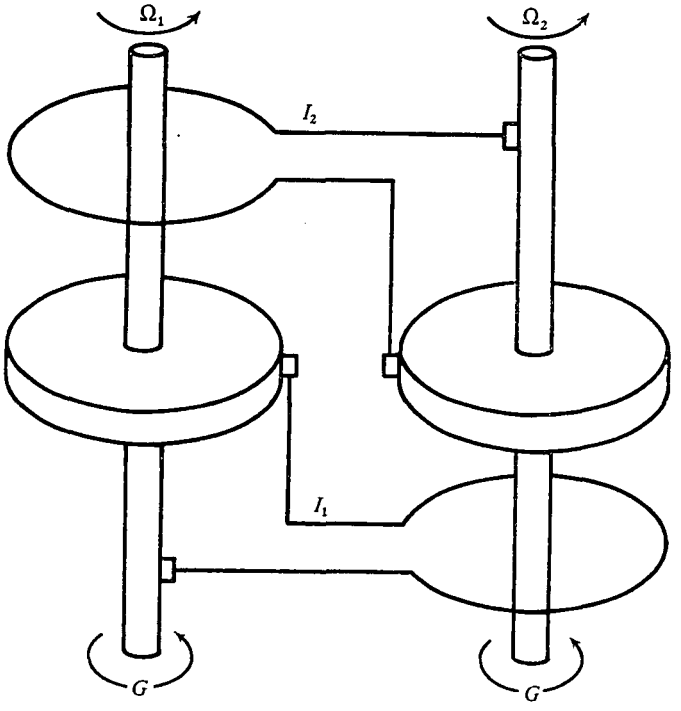


Fig. 1. The Rikitake dynamo.

2. *The Rikitake dynamo.* Rikitake's model, in its simplest form, consists of two identical frictionless disc dynamos connected as shown in Fig. 1. The dynamos are driven by identical torques, G, to maintain their motions in the face of ohmic losses in the coils and discs. The discs of the model may be taken to resemble two large eddies in the Earth's core, each exciting the other after the manner of Herzenberg's dynamo(7).

https://doi.org/10.1017/S0305004100046338 Published online by Cambridge University Press

The torques may be likened to buoyancy forces turning the eddies. The retention of resistive dissipation and the neglect of frictional forces reflect the probable dominance of ohmic diffusion over viscous diffusion in the Earth's core. Although these features of the Rikitake model replicate the Earth faithfully, the model is crude in the sense of neglecting other features such as the diffusive and Alfvénic time delays in the communication between eddies in the core, and the effects of Coriolis forces.

The equations governing the currents I_1 and I_2 and angular velocities Ω_1 and Ω_2 are

$$L\dot{I}_1 + RI_1 = M\Omega_1 I_2, \tag{1}$$

$$L\dot{I}_2 + RI_2 = M\Omega_2 I_1, \tag{2}$$

$$C\dot{\Omega}_1 = G - MI_1 I_2, \tag{3}$$

$$C\dot{\Omega}_2 = G - MI_1 I_2, \tag{4}$$

where L is the self inductance and R the resistance associated with each dynamo and its connecting circuitry, and M is the 'mutual inductance' between the dynamo circuits; C is the moment of inertia of a dynamo about its axis, and G is the couple applied about that axis. It follows from (3) and (4) that the difference in angular velocities is constant

$$\Omega_1 - \Omega_2 = (GL/CM)^{\frac{1}{2}}.A \quad (A = \text{constant}), \tag{5}$$

and when A is assigned there are two steady state solutions

$$I_1 = \pm K(G/M)^{\frac{1}{2}}, \quad I_2 = \pm K^{-1}(G/M)^{\frac{1}{2}}, \quad \Omega_1 = K^2(R/M), \quad \Omega_2 = K^{-2}(R/M). \tag{6}$$

The plus-minus signs in these expressions are to be taken together, and correspond to the normal (N) and reversed (R) states respectively. These labels are arbitrary in the sense that every statement made about transitions between the N and the R state remains true if the letters N and R are interchanged.

The system has two time scales. The first is a 'mechanical time scale', τ_m, and is essentially the time the discs would take to accelerate to the typical angular velocity, R/M, of (6) under the action of the applied couple in the absence of Lorentz forces; that is

$$\tau_m = CR/GM. \tag{7}$$

The second time scale might be termed the 'electromagnetic diffusion time', τ_e; if the discs were stopped with magnetic fields present, these fields would decay, according to (1) and (2), in a typical time of order

$$\tau_e = L/R. \tag{8}$$

An important parameter of the system is the ratio of these times, namely

$$\mu^2 = \frac{\tau_m}{\tau_e} = \frac{CR^2}{GLM}, \tag{9}$$

which is also equal to the ratio of the stored mechanical energy to the stored electromagnetic energy.

The equations are put into non-dimensional form by measuring t in units of $\sqrt{(\tau_e \tau_m)}$,

https://doi.org/10.1017/S0305004100046338 Published online by Cambridge University Press

currents in units of $\sqrt{(G/M)}$, and angular velocities in units of $\sqrt{(GL/CM)}$. Writing

$$I_i = \left(\frac{G}{M}\right)^{\frac{1}{2}} X_i, \quad \Omega_i = \left(\frac{GL}{CM}\right)^{\frac{1}{2}} Y_i, \quad (i = 1, 2) \tag{10}$$

equation (5) becomes

$$Y_1 - Y_2 = A. \tag{11}$$

The governing equations (1) to (3) then become

$$\dot{X}_1 + \mu X_1 = Y X_2, \tag{12}$$

$$\dot{X}_2 + \mu X_2 = (Y - A) X_1, \tag{13}$$

$$\dot{Y} = 1 - X_1 X_2. \tag{14}$$

The steady state solutions (6) become

$$X_1 = \pm K, \quad X_2 = \pm K^{-1}, \quad Y = Y_1 = \mu K^2, \quad Y_2 = \mu K^{-2}, \tag{15}$$

where

$$A = \mu(K^2 - K^{-2}). \tag{16}$$

Without loss of generality, it may be assumed that $A > 0$, i.e. $K > 1$; otherwise the roles of the dynamos are merely reversed. Equations (12) to (14) do not, in general, have known analytic solutions; the only case for which an exact solution is known is $\mu = 0$, $A = 0$ discussed by Allan (5).

Taking τ_m to be the time taken for slow Alfvén waves to cross the core, and assuming a poloidal field of 5 gauss to define the Alfvén velocity, yields $\tau_m = 10^6$ years. Using the above value τ_m, and assuming $\tau_e = 10^4$ years, yields a value $\mu = 10$. Although this procedure conflicts with the definition (7) of τ_m, it does provide a possible estimate of μ. Alternatively, μ may be determined as the ratio of mechanical to magnetic energy densities: using values of these densities, as given by Bullard and Gellman (8) a value of $\mu = 10^{-3}$ is found. Allan (5) and Lowes (reported in (9)) give a value of $\mu = 3 \times 10^{-3}$. Thus, μ in the range 10^{-3} to 10 may be most relevant to the Earth. Assuming a value of $K = 2$ to be representative of the Earth, it is found that a value of μ between 1 and 2 for the Rikitake model would describe the observed reversals most faithfully. It should be admitted, however, that even taking $\tau_m = 10^6$ years and $\tau_e = 10^4$ years, the time scale $\sqrt{\tau_e \tau_m}$ of the process described here is very short compared with the average length of a polarity epoch. It is, then, perhaps unrealistic to draw too close a comparison between the Earth and the present model.

3. *Behaviour near a stationary point.* The solutions infinitesimally close to the steady state N may be found most readily using the transformations

$$U_1 = X_1 - K, \quad U_2 = X_2 - K^{-1}, \quad U_3 = Y - \mu K^2. \tag{17}$$

Substituting from (17) into equations (12) to (14) and using (16) yields Liapounov's first canonical form

$$\dot{U}_i = \sum_{j=1}^{3} q_{ij} U_j + N_i \quad (i = 1, 2, 3), \tag{18}$$

where the q_{ij} are the elements of the matrix

$$Q = (q_{ij}) = \begin{pmatrix} -\mu & \mu K^2 & K^{-1} \\ \mu K^{-2} & -\mu & K \\ -K^{-1} & -K & 0 \end{pmatrix}, \tag{19}$$

https://doi.org/10.1017/S0305004100046338 Published online by Cambridge University Press

and
$$N_1 = U_2U_3, \quad N_2 = U_1U_3, \quad N_3 = -U_1U_2. \tag{20}$$

One of the two steady states of (18) is $U_1 = 0$, $U_2 = 0$, $U_3 = 0$. Neglecting the N_i terms, equation (18) reduces to the linear (abridged) system

$$\dot{U}_i = \sum_{j=1}^{3} q_{ij}U_j \quad (i = 1, 2, 3). \tag{21}$$

The abridged system has the characteristic equation

$$|sI - Q| = 0, \tag{22}$$

which yields the characteristic roots

$$s = -2\mu, \ +i\lambda, \ -i\lambda, \tag{23}$$

where
$$\lambda^2 = K^2 + K^{-2} \geqslant 2.$$

Corresponding to the above roots we have the following solutions:

$$\left.\begin{aligned} U_1 &= C_1 e^{-2\mu t} + C_2 \sin \lambda t + C_3 \cos \lambda t, \\ U_2 &= -C_1 K^{-1} e^{-2\mu t} + C_4 \sin \lambda t + C_5 \cos \lambda t, \\ U_3 &= C \sin \lambda t, \end{aligned}\right\} \tag{24}$$

where C and C_1 are arbitrary constants, and t is chosen so that

$$U_3(0) = 0.$$

The remaining coefficients are given by the identities

$$C_2 = \frac{C\mu(2 - K^2\omega^2)}{K(\omega^2 + 4\mu^2)}, \quad C_3 = \frac{-C\omega(1 + 2\mu^2K^2)}{K(\omega^2 + 4\mu^2)}, \quad C_4 = -\frac{C_2}{K^2}, \quad C_5 = -\frac{CK\omega + C_3}{K^2}.$$

Equations (24) would describe the trajectory of a point in (U_1, U_2, U_3) space, which approaches the plane $U_3 = \alpha_1 U_1 + \alpha_2 U_2$ as t tends to infinity, where

$$\alpha_1 = \frac{K(K^2 + 2\mu^2)}{\mu(1 - K^4)}, \quad \alpha_2 = \frac{K^{-1}(K^{-2} + 2\mu^2)}{\mu(1 - K^{-4})}. \tag{25}$$

Trajectories in the plane would be closed orbits about the point $U_1 = 0$, $U_2 = 0$, $U_3 = 0$. By replacing K by $-K$ in equations (17) the linear solutions about the steady state R can be found. The linearized system yields solutions which ultimately lie arbitrarily close to a limit surface consisting of two planes, one plane passing through the stationary point of the N state, and the other through the stationary point of the R state.

4. *System near the N state.* The question of stability near the stationary point N, and similarly R, cannot be settled by the abridged system (21) because of the form of the characteristic roots (23). Liapounov (10) has examined the stability of systems of equations of the above type, and the following analysis is based on one of his direct methods.

By use of the transformation

$$\begin{pmatrix} U \\ V \\ W \end{pmatrix} = \begin{pmatrix} 0 & 0 & 1 \\ \lambda^{-1}K^{-1} & \lambda^{-1}K & 0 \\ \lambda^{-1}K & -\lambda^{-1}K^{-1} & 0 \end{pmatrix} \begin{pmatrix} U_1 \\ U_2 \\ U_3 \end{pmatrix} \tag{26}$$

https://doi.org/10.1017/S0305004100046338 Published online by Cambridge University Press

and its inverse
$$\begin{pmatrix} U_1 \\ U_2 \\ U_3 \end{pmatrix} = \begin{pmatrix} 0 & \lambda^{-1}K^{-1} & \lambda^{-1}K \\ 0 & \lambda^{-1}K & -\lambda^{-1}K^{-1} \\ 1 & 0 & 0 \end{pmatrix} \begin{pmatrix} U \\ V \\ W \end{pmatrix} \tag{27}$$

(18) is converted into a canonical form of the second kind

$$\left.\begin{aligned} \dot{U} &= -\lambda V - \lambda^{-2}(V^2 - W^2 + \alpha VW) = -\lambda V + \overline{U}, \\ \dot{V} &= \lambda U + \lambda^{-2}U(2V + \alpha W) = \lambda U + \overline{V}, \\ \dot{W} &= \mu(\alpha V - 2W) + \lambda^{-2}U(\alpha V - 2W) = \mu(\alpha V - 2W) + \overline{W}, \end{aligned}\right\} \tag{28}$$

where
$$\alpha = K^2 - K^{-2} \geqslant 0.$$

To examine the stability of (28) the following function is introduced:

$$L = U^2 + V^2 + f(U, V, W), \tag{29}$$

where

$$f = p_1 U^3 + p_2 V^3 + p_3 U^2 W + p_4 V^2 U + p_5 V^2 W + p_6 W^2 U + p_7 W^2 V + p_8 UVW,$$

and
$$\left.\begin{aligned} p_1 &= -\frac{\mu\alpha^2(8\mu^2 + 3\lambda^2)}{3D}, & p_2 &= -\frac{2}{3\lambda^3} + \frac{2\alpha^2\mu^2(\lambda^2 - 4\mu^2)}{3\lambda D}, \\ p_3 &= -\frac{\alpha\lambda(\lambda^2 - 4\mu^2)}{D}, & p_4 &= -\frac{\mu\alpha^2(6\mu^2 + \lambda^2)}{D}, \\ p_5 &= -\frac{\alpha\lambda(6\mu^2 + \lambda^2)}{D}, & p_6 &= \frac{8\mu}{\lambda^2(\lambda^2 + 16\mu^2)}, \\ p_7 &= -\frac{2}{\lambda(\lambda^2 + 16\mu^2)}, & p_8 &= -\frac{2\mu\alpha(\lambda^2 - 4\mu^2)}{D}, \end{aligned}\right\} \tag{30}$$

$$D = \lambda^2(\lambda^2 + \mu^2)(\lambda^2 + 16\mu^2).$$

The coefficients (30) have been chosen (uniquely) so that, in virtue of (28), only quartic terms remain on the right-hand side of

$$\begin{aligned} \dot{L} &= 2U\dot{U} + 2V\dot{V} + \dot{U}\frac{\partial f}{\partial U} + \dot{V}\frac{\partial f}{\partial V} + \dot{W}\frac{\partial f}{\partial W}; \\ &= \overline{U}\frac{\partial f}{\partial U} + \overline{V}\frac{\partial f}{\partial V} + \overline{W}\frac{\partial f}{\partial W}. \end{aligned} \tag{31}$$

The stability of the orbit near the N state is now examined by using the unique linear approximation

$$W = -\frac{\alpha\mu(\lambda U - 2\mu V)}{\lambda^2 + 4\mu^2} \tag{32}$$

in the right-hand side of (31). With this approximation the subsequent analysis holds only for orbits on the N sheet and is not relevant to orbits approaching N from the R sheet during a reversal. Using the transformations

$$U = r\cos\theta, \quad V = r\sin\theta, \tag{33}$$

and substituting for W from (32) into (31)

$$\dot{L} = r^4 H(\theta). \tag{34}$$

https://doi.org/10.1017/S0305004100046338 Published online by Cambridge University Press

According to the Liapounov theory, stability is decided by the sign of the integral

$$G(\mu, K) = \frac{1}{\pi}\int_0^{\pi} H(\theta)\, d\theta. \tag{35}$$

On carrying out the integration it is found that

$$G(\mu, K) = \frac{\mu^3\lambda^2(\lambda^2-2)(\lambda^2+2)}{2(\lambda^2+\mu^2)(\lambda^2+4\mu^2)^2}. \tag{36}$$

It is worth noting that, if $K = 1 (\lambda^2 = 2)$, or $\mu = 0$, solutions exist of the Bullard type in which $X_1 = X_2$. These solutions possess closed trajectories for which G must vanish, and, as may be seen from (36), G is indeed zero for these cases. For all other physically possible K and μ, G is positive, and therefore N is an unstable focus.

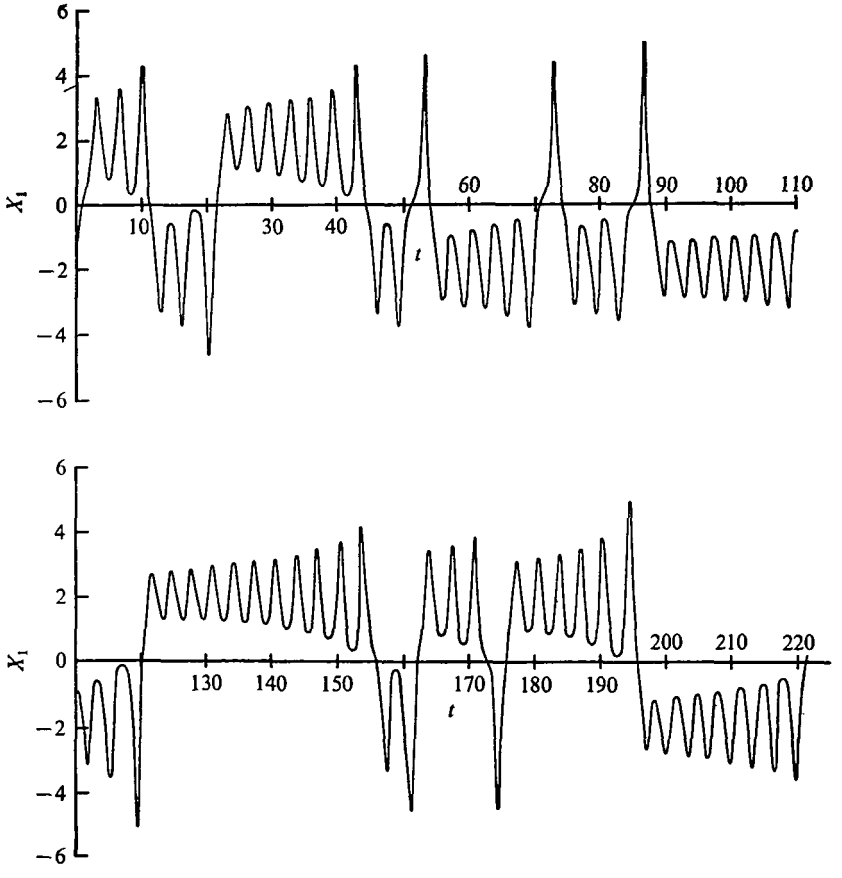


Fig. 2. A typical evolution of X_1 as a function of time, t, for $\mu = 1$, $K = 2$.

5. *Topology of the trajectories in phase space.* In agreement with results of section 4 above, it is found, in all cases in which equations (12) to (14) have been numerically integrated, that no matter how close the system is at one instant of time to state N,

https://doi.org/10.1017/S0305004100046338 Published online by Cambridge University Press

it will systematically depart through oscillations of increasing amplitude to the neighbourhood of the R state. The number of intermediate oscillations may be arbitrarily large if the initial starting point is sufficiently close to N. Fig. 2 illustrates the system behaviour for $\mu = 1$, $K = 2$, and clearly shows reversals taking place at times $t = 11$, 21, 44, 51, 53, 71, 74, 85, etc. Although Fig. 2 is informative, it does not provide the most compact or revealing description of the behaviour of the dynamo. It is more informative to plot the behaviour of the system as an orbiting point in (X_1, X_2, Y) space, or phase space as we shall call it. An ensemble of all such orbits would describe a 'phase fluid' whose Eulerian velocity, $\mathbf{u} = (\dot{X}_1, \dot{X}_2, \dot{Y})$, is, according to (12) to (14), given by

$$\mathbf{u} = [-\mu X_1 + YX_2,\ -\mu X_2 + (Y-A)X_1,\ 1 - X_1X_2]. \tag{37}$$

The specific volume of the phase fluid may be defined by the Jacobian

$$J = \frac{\partial(X_1, X_2, Y)}{\partial(X_{10}, X_{20}, Y_0)}, \tag{38}$$

where the suffix 0 denotes values of these variables at some instant in time. These are Lagrangian co-ordinates for the phase fluid. The equation of continuity in Lagrangian form is

$$DJ/Dt = J \operatorname{div} \mathbf{u},$$

which, using (37), yields the result given by Allan(5)

$$J = e^{-2\mu t}. \tag{39}$$

Thus the volume occupied by any element of phase fluid tends to zero in a time of order $1/\mu$. This strongly suggests the existence of a *limit surface*, S, with the property that, apart from a possible set of measure zero, the points in any such element of phase fluid will ultimately lie arbitrarily close to S. The proviso concerning the set of measure zero is important, as may be seen explicitly by the following example. If the singular trajectory

$$X_1 = X_2 = 0, \quad Y = Bt + C \tag{40}$$

passes through V, points in V and on this trajectory will depart arbitrarily far from the remaining points in V as t tends to infinity. No other singular trajectories are known to us.

Fig. 3 and 4 show the projection of an orbiting point on the (X_2, Y) plane for the case $\mu = 1$, $K = 2$; Fig. 4 is a continuation in time of Fig. 3, the points 2 and 3 of the respective figures corresponding to the same instant of time. As may be seen, there is a region about the N state and about the R state which is not traversed by any trajectory. Although it is possible to start a trajectory within either of these regions, and although such a trajectory may apparently fall onto a surface containing the local stationary point, these regions are actually 'holes' in the limit surface and do not lie on it: an orbit started in either region will spiral outwards until it passes permanently out of the region. In the same way, an orbit started outside the large outer envelope of the orbits will always proceed towards the densely filled regions and remain there. Fig. 5 and 6 are the limit surfaces for the cases $\mu = 1$, $K = 2$, and $\mu = 0{\cdot}6$, $K = 2$

https://doi.org/10.1017/S0305004100046338 Published online by Cambridge University Press

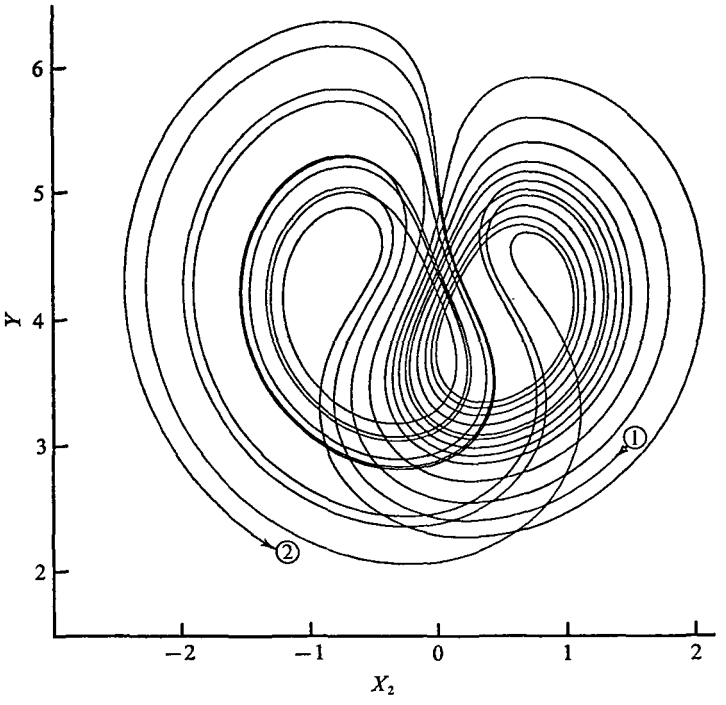


Fig. 3. Projection on the (X_2, Y) plane of a trajectory in phase space for $\mu = 1$, $K = 2$. Points 1 and 2 encircled are explained in the text.

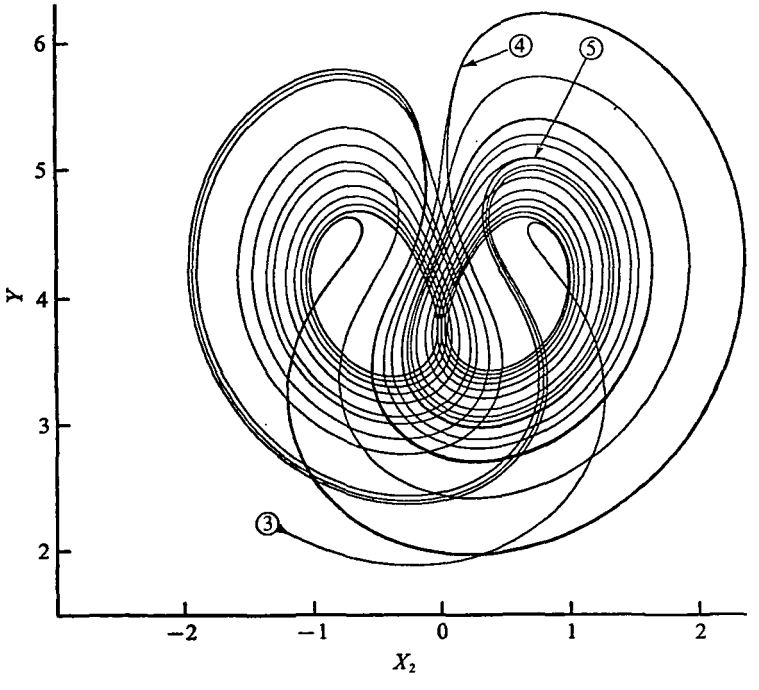


Fig. 4. The continuation of Fig. 3. The encircled point 3 is coincident with point 2 on Fig. 2. For an explanation of points 4 and 5 see text.

https://doi.org/10.1017/S0305004100046338 Published online by Cambridge University Press

respectively. The limit surface appears to consist of two sheets, an upper right-hand sheet and a lower left-hand sheet; the boundaries of the latter are shown as broken lines when they lie below the former. The right-hand inner loop surrounds the N state, $(K, K^{-1}, \mu K^2)$, and the left-hand inner loop surrounds the reverse R state, $(-K, -K^{-1}, \mu K^2)$. The outer boundaries of the left-hand and right-hand sheets are each part of a trajectory, whilst the inner loops surrounding the N and R states are not. The region between the outer loop and the two inner loops is, in projection, fairly uniformly traversed by the orbiting point, although there is a higher density of occupation near the inner loops, and in the vicinity of the nearly periodic solutions. The solutions of (12) to (14) cannot, of course, meet or touch, but there are instances in which they appear to merge (e.g. points 4 and 5 on Fig. 4). It is important for this reason to distinguish between the projection S_p of an orbit near S onto that surface, and S itself. It is not possible in practice to study an orbit which lies precisely on S, but if one could do so, it would be found that such an orbit could not pass from one sheet to the other without violating (12) to (14).

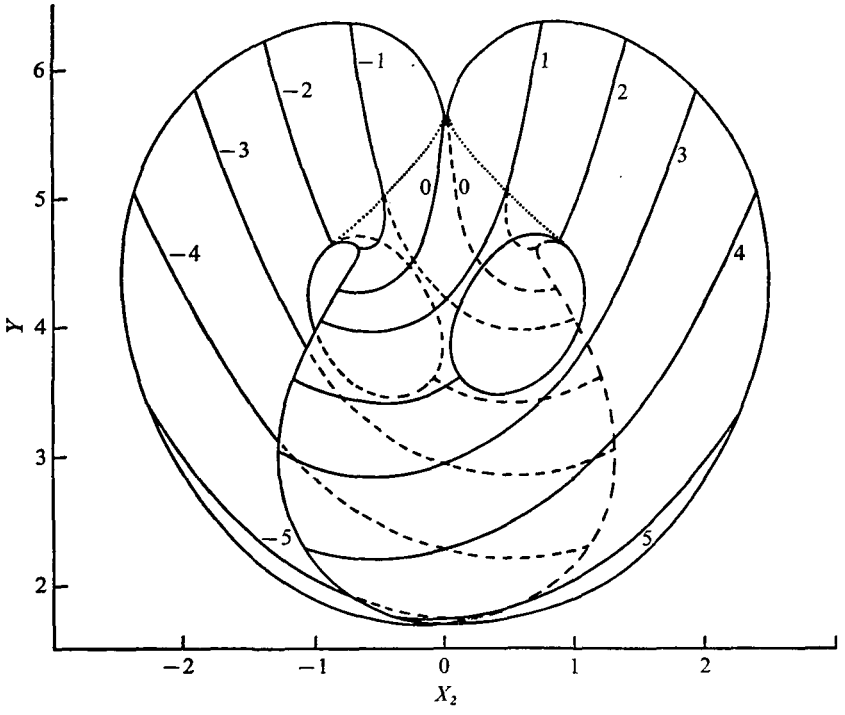


Fig. 5. The limit surface for $\mu = 1$, $K = 2$. The contour lines on the surface are of constant X_1. The dotted lines are apparent lines of contact of the two sheets.

Topologically S_p appears, as Figs. 5 and 6 indicate, to be a finite simplicial complex not containing fixed points under the transformation group g defined by the differential equations (12) to (14). Fig. 7 presents a schematic idealization of S_p. The ray AB on the left is identified with the arc AB on the right, and the arc BC on

https://doi.org/10.1017/S0305004100046338 Published online by Cambridge University Press

the left with the ray BC on the right. The orbit passes from one sheet to the other via these common curves. The surface illustrated in Fig. 7 belongs to the same homotopy class as a wedge of two circles, and its fundamental group is the free group on two generators. (It is, in fact, amusing to regard each orbit, over a sufficiently large time interval, as an element of this group.)

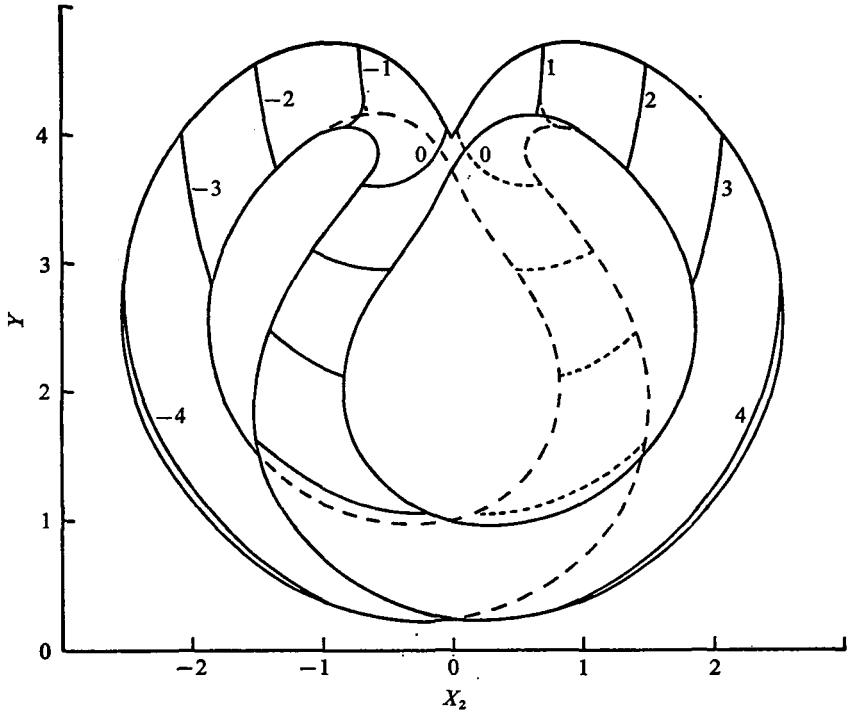


Fig. 6. The limit surface for $\mu = 0{\cdot}6$, $K = 2$. See caption to Fig. 5 for further explanation.

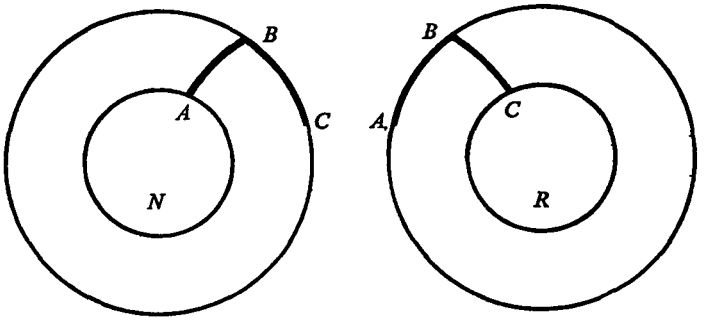


Fig. 7. Schematic form of limit surface, S_p. The arcs AB on each sheet should be identified with each other, likewise for arcs BC.

It is important to recognize that S cannot be of this form: for if it were, the zero and one dimensional betti numbers would be 1 and 2 respectively, and the Euler–Poincaré index of the surface would be non-zero (-1). The transformation on S defined by g is,

https://doi.org/10.1017/S0305004100046338 Published online by Cambridge University Press

however, homotopic to 1_S. It follows, by Lefschetz's fixed point theorem, that contrary to supposition, S_p would contain fixed points. The identification of AB and CD on the left and right of Fig. 7 is therefore not possible for S, and orbits cannot cross from one sheet to the other. Once placed (precisely!) on S, the orbit would remain encircling the corresponding N or R state for all time, either describing closed orbits or spiralling towards a limit cycle at the inner or outer boundaries of the sheet concerned.

A set of differential equations similar to (12) to (14), with a property analogous to (39), has been studied by Lorenz (11). The isopleth of solutions which he has constructed is similar in form to our limit surfaces.

6. *Numerical results.* Diagrams showing trajectories of the orbiting point were obtained from numerical results of a fourth order Runge–Kutta method, although a considerable amount of exploratory work was carried out on an analogue computer. The numerical integrations were carried out for times of order 200 to 500 units, so as to define the limit surface with sufficient precision, as well as to obtain reasonable estimates for the average number of oscillations between reversals. The authors know of no other investigation, with the exception of some unpublished results of F. J. Lowes, in which the integrations have been so extensive in time. Except where explicitly stated otherwise, the discussion below refers to $K = 2$ cases.

For the case $\mu = 1$, the number of oscillations between reversals ranges from 1 to 11, with an average of about 4. If the orbit just reaches the R sheet from the N sheet, it will do so high up the dotted curve well removed from the R state (see Fig. 5), and will therefore return almost immediately to the N sheet. Such a reversal corresponds to the polarity event of Cox (1). If the orbit leaves the N sheet near the boundary, it will reach the R sheet on that part of the dotted curve close to the R state. Subsequently, a large number of oscillations will occur before the orbit reverses back to the N sheet: this corresponds to Cox's polarity epoch.

Some of the statistical information about the reversal behaviour may be summarized as follows. Let X_{1m} denote the largest value of X_1 which occurs during the cycle of the N loop immediately prior to the reversal to the R sheet. The number of oscillations, N_{osc}, it executes in that state before reverting to its original polarity is given by the integral part of

$$N_{\text{osc}} = a(\mu, K)[|X_{1m}| - b(\mu, K)]. \tag{41}$$

(The functions a and b are, of course, unchanged when K is replaced by K^{-1}.) With $\mu = 1$, it is found that $a \simeq 10$ and $b \simeq 4$; and with $\mu = 0{\cdot}6$, $a \simeq 3$ and $b \simeq 3{\cdot}6$.

The average number of oscillations, A_v, between reversals is shown in Fig. 8 and 9. There appears to be a global maximum for A_v at $\mu = 1$, $K = 2$.

A search for purely periodic solutions was made employing a modified Davidon method (Davidon (12), Fletcher and Powell (13)) based on the minimization of the function

$$F^2 = [X_1(\tau) - X_1(0)]^2 + [X_2(\tau) - X_2(0)]^2 + [Y(\tau) - Y(0)]^2 \tag{42}$$

for solutions close to the stationary points. F may be considered as a measure of the increment in 'distance' of the trajectory from the state N on completion of one orbit

https://doi.org/10.1017/S0305004100046338 Published online by Cambridge University Press

about N. The initial distance of the trajectory from the state N may be defined by

$$D^2 = [X_1(0) - K]^2 + [X_2(0) - K^{-1}]^2 + [Y(0) - \mu K^2]^2. \tag{43}$$

The minimization of F^2 is performed over the initial values $X_1(0)$, $X_2(0)$ and $Y(0)$ and over τ as independent variables. τ is closely approximated by the period $2\pi(K^2 + K^{-2})^{-\frac{1}{2}}$ as given by the linear theory.

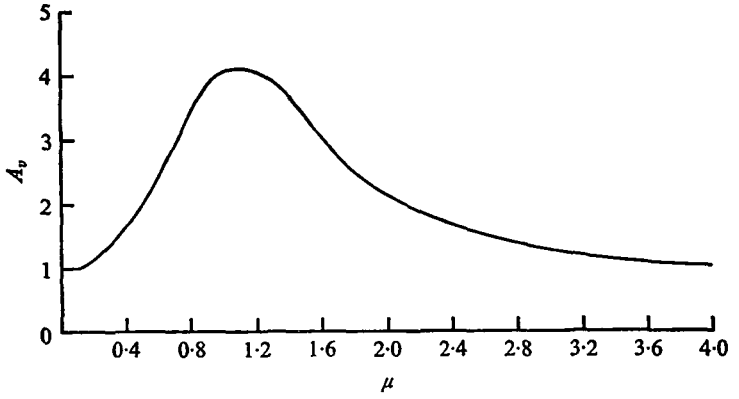


Fig. 8. The average number, A_v, of oscillations between reversals, as a function of μ for $K = 2$.

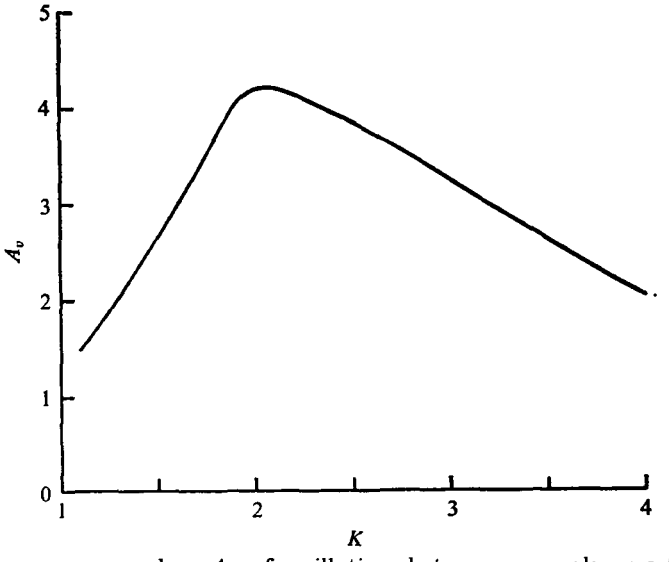


Fig. 9. The average number, A_v, of oscillations between reversals, as a function of K for $\mu = 1$.

Fig. 10 is a plot of the minimum value of F against D for the case $\mu = 0{\cdot}5$. For values of $D < 0{\cdot}4$ it is found that F depends on $D^{4{\cdot}2}$ approximately, a result in good agreement with that obtained by the stability theory. For large values of D ($> 0{\cdot}4$) the dependence of F upon D becomes more nearly linear. It follows from Fig. 10 that trajectories which start close to the N state will spiral outward slowly at first and then more rapidly as D increases.

https://doi.org/10.1017/S0305004100046338 Published online by Cambridge University Press

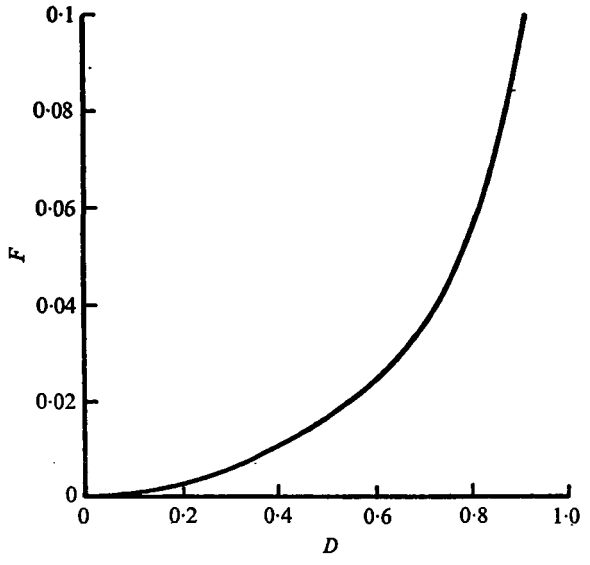


Fig. 10. The minimum value of F obtained during the search for periodic solutions at a 'distance', D, from a stationary point.

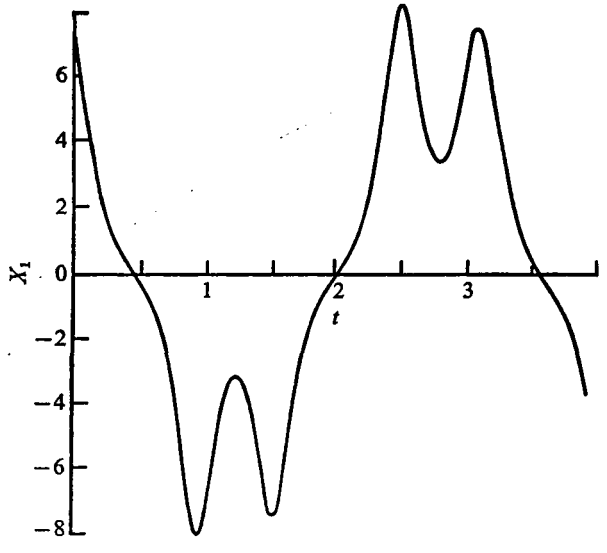


Fig. 11. A nearly periodic orbit for $\mu = 0{\cdot}1$, $K = 2$, having a single oscillation about each stationary point between reversals. (Time evolution.)

In the search for periodic solutions in which a reversal takes place, the function

$$F^2 = [X_1(\tau) + X_1(0)]^2 + [X_2(\tau) + X_2(0)]^2 + [Y(\tau) - Y(0)]^2 \tag{44}$$

is to be minimized.

The difference in sign in the brackets of (44) arises from the consideration that singly periodic solutions of X_1 and X_2 would necessarily imply doubly periodic solutions in Y.

https://doi.org/10.1017/S0305004100046338 Published online by Cambridge University Press

Estimates of $X_1(0)$, $X_2(0)$, $Y(0)$ and τ were obtained from lengthy integrations performed for the limit surface.

The presence of a zero F for (44) would imply periodic reversal solutions; however, there was no evidence that such solutions exist. Local minima were found corresponding to 'almost periodic' solutions of a greater (small F) or lesser (large F) degree of permanence. For small μ (of order 0·1 or less), only one minimum was found; an example is shown in Figs. 11 and 12, for the case $\mu = 0{\cdot}1$. Despite appearances, the trajectory performs only one excursion about the stationary point before reversing to the other. For these values of μ any trajectory, irrespective of its starting point, eventually reduces to this periodic orbit and repeats it faithfully over a large number

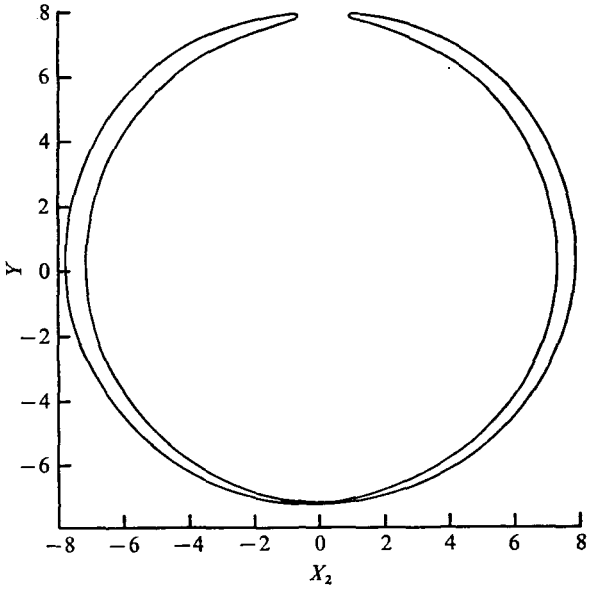


Fig. 12. As Fig. 11 except that the orbit is shown in projection on the (X_2, Y) plane.

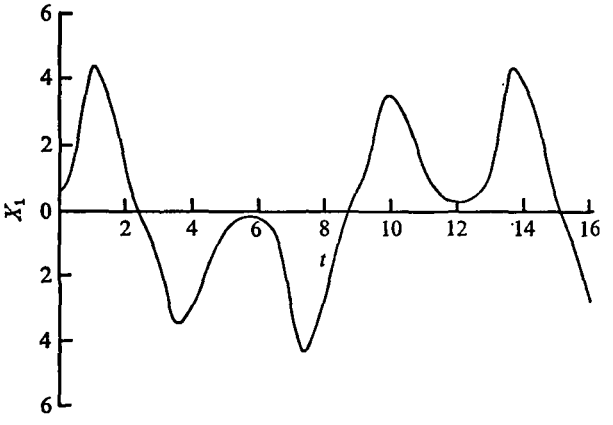


Fig. 13. A nearly periodic orbit for $\mu = 0{\cdot}6$, $K = 2$, having a double oscillation about each stationary point between reversals. (Time evolution.)

https://doi.org/10.1017/S0305004100046338 Published online by Cambridge University Press

of cycles. For large μ (e.g. $\mu = 4$) the same kind of behaviour appears to be true. For the intermediate value $\mu = 0{\cdot}6$ two minima were found, one in which reversal takes place after a double oscillation, and the other in which the reversal takes place after a single oscillation. The double oscillation, of considerable persistence, is shown in Figs. 13 and 14. The single oscillation, also fairly persistent, is shown in Figs. 15 and 16.

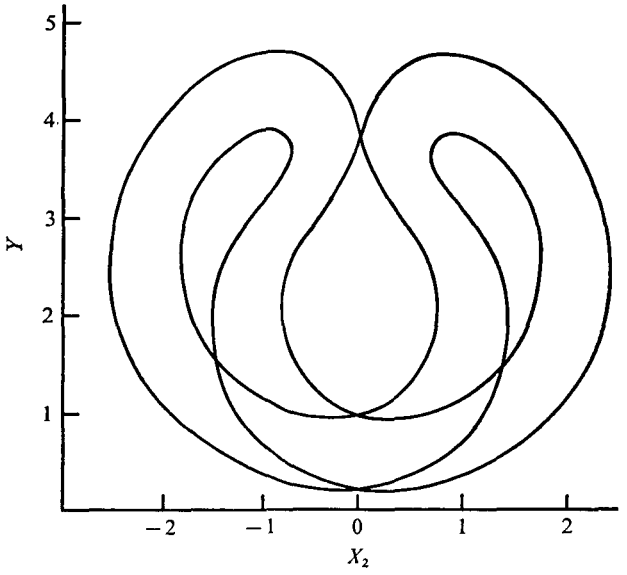


Fig. 14. As Fig. 13 except that the orbit is shown in projection on the (X_2, Y) plane.

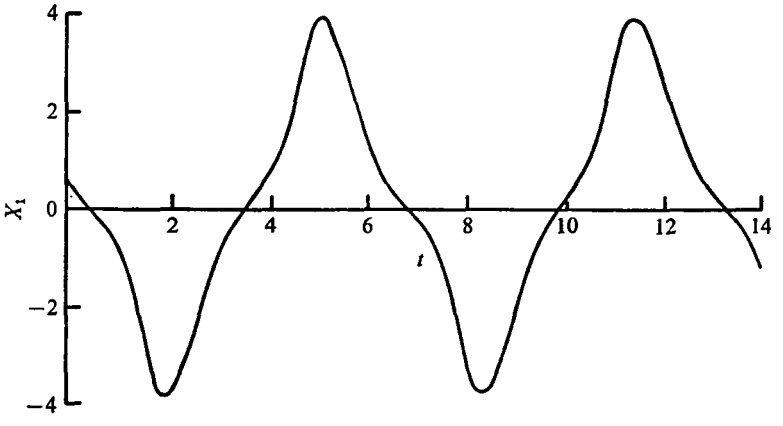


Fig. 15. A nearly periodic orbit for $\mu = 0{\cdot}6$, $K = 2$, having a single oscillation about each stationary point between reversals. (Time evolution.)

Three additional integrations were performed with $\mu = 1$ and $A = 0{\cdot}1$, $0{\cdot}01$ and $0{\cdot}001$. The solutions, particularly for the smaller A values, exhibit almost regular reversals with one oscillation between reversals. The form of the solution, excepting the reversal phase, closely follows that of the single disc Bullard dynamo. The period, P,

https://doi.org/10.1017/S0305004100046338 Published online by Cambridge University Press

and the maximum value of $\frac{1}{2}(X_1+X_2)$, denoted by α, are related to the first-order approximation by

$$P = 2\alpha + (2/\alpha)\log 2. \tag{45}$$

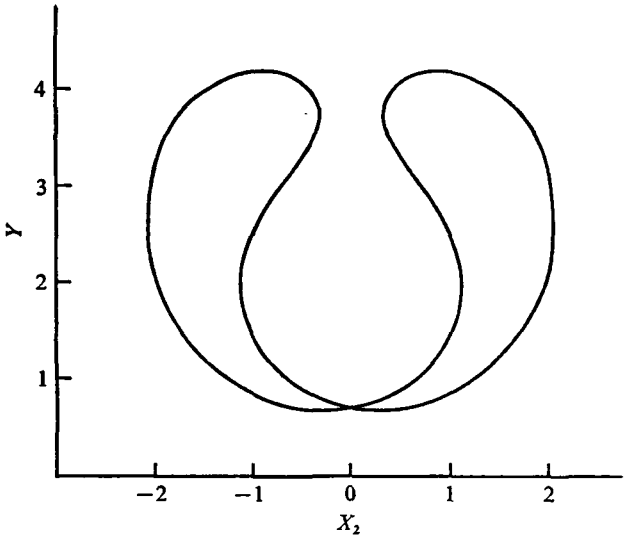


Fig. 16. As Fig. 15 except that the orbit is shown in projection on the (X_2, Y) plane.

The following table compares the computed period as given by (45) with that obtained by the method described above for periodic solutions:

μ	A	P	Computed P
1	0·1	7·86	7·77
1	0·01	9·13	9·15
1	0·001	10·50	10·48

Although the above table shows a good agreement between the computed and actual period (45) it is not as satisfactory for the small dissipation cases in which A may be quite large. For such cases the relationship between period P, α and A is given approximately by:

$$A = 8\alpha e^{-\frac{1}{4}\alpha P}. \tag{46}$$

For $K = 2$, $\mu = 0{\cdot}01$, (46) yields a result for P within 7 % of the observed value.

APPENDIX: THE RIKITAKE DYNAMO FOR SMALL A

It has already been noted (6) that, for K fixed, the orbit for sufficiently small μ is closely periodic and has a single oscillation between reversals. This raises the interesting possibility that it might be regarded as an approximation to an exactly periodic orbit obtained from the asymptotic theory for $A \to 0$. A necessary preliminary to the discussion of this idea is the examination of the Bullard single disc dynamo and the associated antidynamo.

The Bullard dynamo. The Bullard (3) single disc dynamo is governed by the differential equations

$$\dot{U} = ZU, \tag{A 1}$$

$$\dot{Z} = 1 - U^2. \tag{A 2}$$

https://doi.org/10.1017/S0305004100046338 Published online by Cambridge University Press

Here U represents current, and $Z = Y - \mu$ represents difference between angular velocity, Y, and the effect of ohmic dissipation, μ. The phase diagram defined by the dynamo is shown in Fig. 17. It may be noted that U always retains its initial sign. Suppose that $U > 0$. If α (> 1) denotes the maximum value of U on one of the curves shown, the curve itself is given, from (A 1) and (A 2), by

$$Z^2 = \alpha^2 - U^2 + 2\log(U/\alpha). \tag{A 3}$$

In addition to the maximum ($U = \alpha$, $Z = 0$) the curve possesses a minimum U, viz.

$$U = \gamma, \quad Z = 0. \tag{A 4}$$

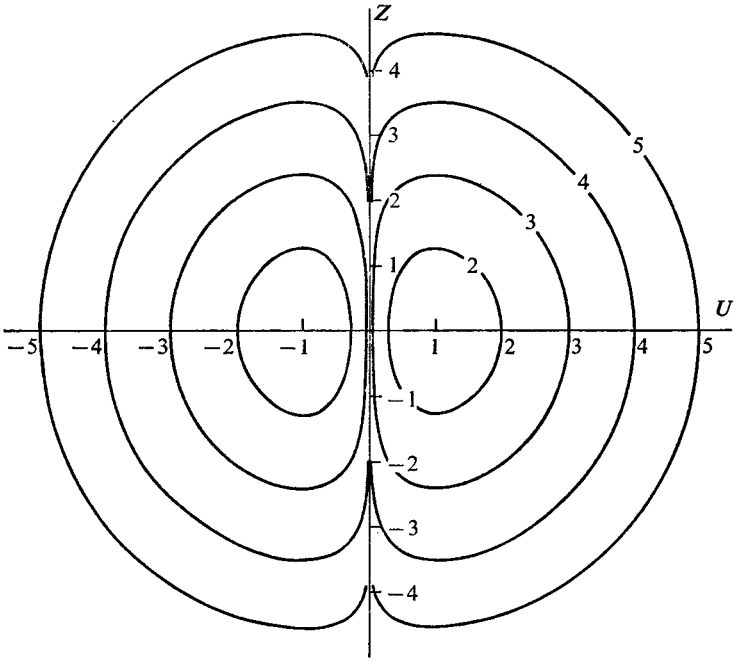


Fig. 17. Phase space solutions for the Bullard dynamo.

For $\alpha \to \infty$, (A 3) yields the asymptotic formula

$$\gamma = \alpha e^{-\frac{1}{2}\alpha^2}(1 + \tfrac{1}{2}\alpha^2 e^{-\alpha^2} + \ldots). \tag{A 5}$$

From (A 1) and (A 3), the time taken by the representative point to complete one of the orbits shown in Fig. 17 is

$$P = 2\int_{\gamma}^{\alpha} \frac{dU}{U[\alpha^2 - U^2 + 2\log(U/\alpha)]^{\frac{1}{2}}}. \tag{A 6}$$

For small $(\alpha - 1)$, the curve is a circle, centred on the equilibrium point ($U = 1$, $Z = 0$), and the representative point describes this circle uniformly. The period of the corresponding simple harmonic motion is $\pi\sqrt{2}$. For $\alpha \gg 1$ the motion around the curve is by no means uniform. It is found that $P \sim 2\alpha$, corresponding to almost uniform motion with unit velocity along the section of curve close to the Z axis; the remainder of the curve is described in a time of order α^{-1}.

https://doi.org/10.1017/S0305004100046338 Published online by Cambridge University Press

The case $\alpha \gg 1$ can be treated by the method of matched asymptotic expansions. For $U \ll 1$, (A 1) and (A 3) may be combined to yield the first-order approximation

$$\frac{dU}{dt} = \pm U[\alpha^2 + 2\log(U/\alpha)]^{\frac{1}{2}}, \tag{A 7}$$

where the sign taken is that of Z. Equation (A 4) may be used to define values of U and Z at time $t = 0$, with this origin the integration of (A 7) gives

$$U = \alpha e^{-\frac{1}{2}\alpha^2} + \tfrac{1}{2}t^2. \tag{A 8}$$

Successive terms in the series expansion of U can be readily obtained by iteration. The second-order approximation is given by

$$U = \alpha e^{-\frac{1}{2}\alpha^2 + \frac{1}{2}t^2} + \tfrac{1}{2}\alpha^3 e^{-\frac{3}{2}\alpha^2 + \frac{3}{2}t^2}\left[1 - 2te^{-t^2}\int_0^t e^{t^2}dt\right]. \tag{A 9}$$

For $U \gg 1$, (A 1) and (A 3) give the first-order approximation

$$dU/dt = \pm U(\alpha^2 - U^2)^{\frac{1}{2}}, \tag{A 10}$$

where the sign taken is again that of Z. The solution of this first-order approximation is

$$U = \alpha \operatorname{sech} \nu, \tag{A 11}$$

where

$$\nu = (t - t_0), \tag{A 12}$$

and $t_0 (= \frac{1}{2}P)$ is the instant at which the maximum ($U = \alpha, Z = 0$) is attained. As before, higher-order approximations can be readily obtained by iteration, the second-order approximation being

$$U = \alpha \operatorname{sech} \nu\left[1 + (1/\alpha^2)\left\{\nu \tanh \nu - \log(\cosh \nu) + \tanh \nu \int_0^\nu \log(\cosh \nu)d\nu\right\}\right]. \tag{A 13}$$

The semi-period, t_0, may be found to the first-order by matching (A 8) to (A 11), or to the second-order by matching (A 9) to (A 13). Substituting (A 12) into (A 8) yields

$$U = \alpha e^{\frac{1}{2}(t_0^2 - \alpha^2)} + \frac{t_0}{\alpha} + \frac{\nu^2}{2\alpha^2}. \tag{A 14}$$

Since $t_0 = O(\alpha)$, then (A 14) to first-order is given by

$$U \sim \alpha \exp[\tfrac{1}{2}(t_0^2 - \alpha^2) + (t_0/\alpha)\nu]. \tag{A 15}$$

From (A 11), as $\nu \to \infty$,

$$U \sim 2\alpha e^{\nu}. \tag{A 16}$$

Expressions (A 15) and (A 16) match if

$$t_0 = \alpha + (1/\alpha)\log 2. \tag{A 17}$$

Similarly, matching (A 9) and (A 13) gives

$$t_0 = \alpha + (1/\alpha)\log 2 + (1/\alpha^3)[(\log 2)^2 + 4\log 2 - 3]. \tag{A 18}$$

The antidynamo. By reversing the connexions of the Bullard dynamo, or by reversing the direction in which the dynamo is driven, the equations of motion corresponding

https://doi.org/10.1017/S0305004100046338 Published online by Cambridge University Press

to (A 1) and (A 2) become

$$\dot{U} = -ZU, \tag{A 19}$$

$$\dot{Z} = 1 + U^2, \tag{A 20}$$

where $Z = Y + \mu$. The solutions in phase space are shown in Fig. 18, and extended to infinity in the $\pm Z$ directions, unlike the closed curves of the Bullard dynamo. If $(U = \alpha, Z = 0)$ is the point at which the curve crosses the U axis, then corresponding to (A 3)

$$Z^2 = \alpha^2 - U^2 - 2\log(U/\alpha). \tag{A 21}$$

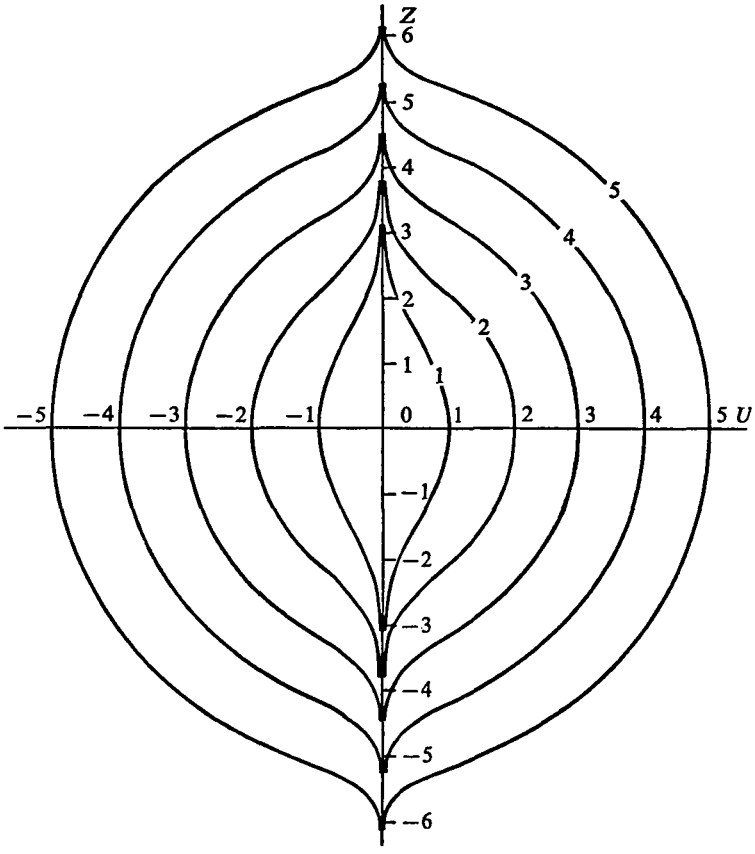


Fig. 18. Phase space solutions for the antidynamo.

The first-order term of the 'inner' expansion for $U \gg 1$ is identical to (A 11), whilst the first-order term of the 'outer' expansion is now

$$U = \alpha e^{\frac{1}{2}\alpha^2 - \frac{1}{2}t^2}, \tag{A 22}$$

the origin of t no longer having the special significance as for the Bullard dynamo.

The coupled dynamos. The coupled dynamo equations (12) and (13) may be replaced by the more symmetrical forms

$$\dot{X}_1 = -\mu X_1 + (Y + \beta) X_2, \tag{A 23}$$

$$\dot{X}_2 = -\mu X_2 + (Y - \beta) X_1, \tag{A 24}$$

https://doi.org/10.1017/S0305004100046338 Published online by Cambridge University Press

$$\dot{Y} = 1 - X_1 X_2, \tag{A 25}$$

where $\beta = \frac{1}{2}A$ and Y represents a scaled $\frac{1}{2}(\Omega_1 + \Omega_2)$, rather than the scaled Ω_1 as in the main text.

Consider the functions U_1 and U_2 defined by the equations

$$X_1 = U_1 - U_2, \quad X_2 = U_1 + U_2. \tag{A 26}$$

Substituting from (A 26) into (A 23), (A 24) and (A 25) yields

$$\dot{U}_1 = (Y - \mu)U_1 + \beta U_2, \tag{A 27}$$

$$\dot{U}_2 = -(Y + \mu)U_2 - \beta U_1, \tag{A 28}$$

$$\dot{Y} = 1 - U_1^2 + U_2^2. \tag{A 29}$$

There are two distinct families of solutions corresponding to $\beta = 0$. For the first of these set U_2 zero; U_1 and $Y - \mu$ are then governed by equation (A 27) and (A 29) which now become the Bullard equations. For the second family, set U_1 zero; then U_2 and $Y + \mu$ obey (A 28) and (A 29) which have reduced to the antidynamo equations. For β small but non-zero, solutions to (A 27) and (A 29) exist in which the following three phases can be distinguished:

(*a*) U_1 large, U_2 small. U_1 and Y very rapidly as in the 'inner' solution of the Bullard equations; U_2 is determined by them.

(*b*) U_1 small, U_2 large. U_2 and Y vary rapidly as in the 'inner' solution of the antidynamo equations; U_1 is determined by them.

(*c*) Y large and slowly varying, U_1 and U_2 intermediate in magnitude by growing or decreasing exponentially.

(The adjectives 'large' and 'small' used here refer to the modulus of the quantity concerned.)

The periodic solution sought consists of two episodes of (*a*) and (*b*), one of each sign and each lasting a time of order α^{-1}. α is to be determined from theory, and corresponds to the amplitude of U_1 for episode (*a*) and to the amplitude of U_2 for episode (*b*). Each passage from phase (*a*) to phase (*b*) is separated by phase (*c*). Consider a half period in which the phases (*a*), (*c*), (*b*) and (*c*) act in succession, commencing at $t = 0$ with a state in which U_1 is maximum and Y and U_2 are zero. (Here, and elsewhere, μ is neglected in comparison with Y.)

In phase (*a*), U_1 and Y are given to the first-order approximation by

$$U_1 = \alpha \operatorname{sech} \alpha t, \quad Y = -\alpha \tanh \alpha t. \tag{A 30}$$

According to (A 28), U_2 is then given to first-order by the appropriate solution of

$$\dot{U}_2 - (\alpha \tanh \alpha t)U_2 = -\alpha\beta \operatorname{sech} \alpha t,$$

namely

$$U_2 = -\beta \sinh \alpha t. \tag{A 31}$$

Clearly, as $\alpha t \to \infty$, i.e. phase (*c*) is entered for the first time, the following approximations hold

$$U_1 \sim 2\alpha e^{-\alpha t}, \quad U_2 \sim -\tfrac{1}{2}\beta e^{\alpha t}, \quad Y \sim -\alpha. \tag{A 32}$$

https://doi.org/10.1017/S0305004100046338 Published online by Cambridge University Press

(A 32) continues to hold during phase (c), to the first approximation. If the duration of this phase is τ, the amplitude of U_1 decreases by a multiple of $\exp(-\alpha\tau)$, while U_2 increases (in magnitude) by a multiple of $\exp(\alpha\tau)$. If the origin of t is now redefined to correspond to the epoch of maximum $-U_2$ in the succeeding phase (b), then for this phase as $\alpha t \to -\infty$

$$U_1 \sim (2\alpha e^{-\alpha\tau})e^{-\alpha t}, \quad U_2 \sim (-\tfrac{1}{2}\beta e^{\alpha\tau})e^{\alpha t}, \quad Y \sim -\alpha. \tag{A 33}$$

In phase (b), U_2 dominates U_1 and, according to the antidynamo theory developed earlier, (A 30) is replaced by

$$U_2 = \alpha \operatorname{sech} \alpha t, \quad Y = \alpha \tanh \alpha t. \tag{A 34}$$

Substituting for U_2 and Y from (A 34) into (A 27) yields

$$U_1 = \beta \sinh \alpha t, \tag{A 35}$$

replacing (A 31).

(A 34) and (A 35) match with (A 33) for $\alpha t \to \infty$ if, and only if

$$e^{\alpha\tau} = 4\alpha/\beta. \tag{A 36}$$

From (A 36) the period p, amplitude α, and A are related by

$$A = 8\alpha e^{-\frac{1}{4}\alpha P}. \tag{A 37}$$

The assumption that Y is constant during phase (c) would appear to contradict (A 29). In detail this is true; however, the net change in Y during this phase is, from (A 29),

$$\Delta Y = \int_0^\tau (1 - U_1^2 + U_2^2)\,dt, \tag{A 38}$$

where the origin of t has reverted to the original definition. From (A 32) the dominant contribution to Y is $O(\alpha)$ and is given by

$$\begin{aligned} \Delta Y &= \tau + \tfrac{1}{2}\alpha[(2\alpha e^{-\alpha t})^2 + (\tfrac{1}{2}\beta e^{\alpha t})^2]_0^\tau, \\ &\sim -2\alpha + \tfrac{1}{2}\alpha(\tfrac{1}{2}\beta e^{\alpha\tau})^2, \end{aligned} \tag{A 39}$$

which vanishes by virtue of (A 36). The change in Y during phase (c) is therefore $O(1) \ll O(\alpha)$, as required.

Only one relationship between the two unknowns α and P is given by (A 37). It is clear from the relations

$$P = 2\oint (U_1^2 - U_2^2)\,dt \tag{A 40}$$

and

$$\oint Y\,dt = \mu \oint (U_1^2 + U_2^2)\,dt, \tag{A 41}$$

(obtained from (A 27) and (A 29)) that before P can be evaluated, the symmetrical structure of the first-order solutions must be broken.

The authors are grateful to Professor G. Horrocks for his contribution to the topological description of the limit surface. We also wish to thank Mr J. Dobson for all the exploratory analogue work and his general interest in this study, and Dr F. J. Lowes for his comments.

https://doi.org/10.1017/S0305004100046338 Published online by Cambridge University Press

REFERENCES

(1) Cox, A. J. *Geophys. Res.* **73** (1968), 3247.
(2) Irving, E. *Paleomagnetism and its application to geological and geophysical problems* (Wiley; New York, 1964).
(3) Bullard, E. C. *Proc. Cambridge Philos. Soc.* **51** (1955), 744.
(4) Rikitake, T. *Proc. Cambridge Philos. Soc.* **54** (1958), 89.
(5) Allan, D. W. *Proc. Cambridge Philos. Soc.* **58** (1962), 671.
(6) Somerville, R. C. J. *Woods Hole Oceanographic Institution, Report* 67–54, vol. II, 132.
(7) Herzenberg, A. *Philos. Trans. Roy. Soc. London, Ser.* A **250** (1958), 543.
(8) Bullard, E. C. and Gellman, H. *Philos. Trans. Roy. Soc. London, Ser.* A **247** (1954), 213.
(9) Hide, R. and Roberts, P. H. *Rev. Modern Phys.* **32** (1960), 799.
(10) Liapounov, A. M. *Problème Générale de la Stabilité du mouvement.* (Annals of Mathematics Studies Number 17, Princeton University Press, 1947.)
(11) Lorenz, E. N. J. *Atmos. Sci.* **20** (1963), 130.
(12) Davidon, W. C. *A.E.C. Research and Development Report* ANC-5990 (Rev.).
(13) Fletcher, R. and Powell, M. J. D. *Comp. J.* **6** (1963), 163.

https://doi.org/10.1017/S0305004100046338 Published online by Cambridge University Press